A NOVEL LINEAR EM RECONSTRUCTION ALGORITHM WITH PHASELESS DATA

H. Zheng, M. Z. Wang, and Z. Q. Zhao

School of Electronic Engineering
University of Electronic Science and Tecnology of China
No. 4, Section 2, North Jianshe Road, Chengdu, China

L. L. Li

Texas A&M University
College Station, Texas 77843, USA

Abstract—This paper presents a fast and effective electromagnetic reconstruction algorithm with phaseless data under weak scattering conditions. The proposed algorithm is based on the phaseless data multiplicative regularized contrast sources inversion method (PD-MRCSI). We recast the weak scattering problem as an optimization problem in terms of the undetermined contrast and contrast sources. Using the conjugate gradient iterative method, the problem is solved by alternately updating the contrast sources and the contrast. Additionally, this method can combine with the PD-MRCSI method. Taking advantage of the properties of fast convergence of this algorithm and stable convergence of PD-MRCSI method, the combined technique makes image reconstructions more fast and effective. Although the method is derived from weak scattering situation, it is also useful for the case which weak scattering approximation is not satisfied. The synthetic numerical reconstruction results, as well as experimental reconstruction results, presented that the proposed method is a very fast and effective reconstruction algorithm.

1. INTRODUCTION

Electromagnetic inverse scattering has found widespread applications in target identification, non-destructive testing, medical imaging and numerous other areas of applications. However, the inverse scattering

---

Corresponding author: H. Zheng (huberyzheng@gmail.com).

problem is commonly nonlinear and ill-posed. Over the years, various effective algorithms, for examples [1–14], have been proposed to solve this involved inverse problem with full data (amplitude plus phase) in different application backgrounds.

In several applied sciences areas, it is difficult or very expensive to measure the phase of the field. Additionally, in many situations, the phase of the field is easier to be polluted by the noise than the amplitude. To overcome it, some approaches which can solve the inverse problem without phase information have been proposed in both optics and electromagnetics [15–18]. Among them, the phaseless data multiplicative regularized contrast sources inversion method (PD-MRCSI) has been found to be an efficient algorithm for inverse scattering problem with phaseless data [19, 20].

The main bottleneck in solving inverse scattering problems with phaseless data is that repeated 'exact' filed computations require an excessive amount of computation time. As it is known, when dealing with weak scatterers, the Born approximation may be used advantageously in many inversion algorithms. Here the Born approximation is introduced in the PD-MRCSI method (PDB-MRCSI), which can degenerate the nonlinear inverse problem into a linear one and reduces the computation time drastically. Taking advantage of the properties of fast convergence of PDB-MRCSI and stable convergence of PD-MRCSI method, the combined technique makes image reconstructions more fast and effective. Although the method is derived from weak scattering situation, it is also useful for the case which weak scattering approximation is not satisfied.

2. PDB-MRCSI METHOD DESCRIPTION

To illustrate the inversion method, we consider a two-dimensional problem shown in Fig. 1. Scattering objects with unknown location and contrast are illuminated by emitter from k ($k = 1, 2, \ldots, K$) different locations distributed evenly around the object domain D. The receivers are distributed in the observation domain S. The complex time factor $\exp(-i\varpi t)$ is employed in this paper, where ϖ is the angular frequency. For weak scattering or Born approximation, the direct scattering problem can be modeled via two coupled contrast source integral relationship, in particular, the data equation and the state equation, explicitly,

$$f_k(r) = u_k^{inc}(r) + k_b^2 \int_D G(r, r') \omega_k(r') dr' \quad \text{for } r \in S \qquad (1)$$

$$u_k(r) = u_k^{inc}(r) \qquad\qquad\qquad\qquad \text{for } r \in D \qquad (2)$$
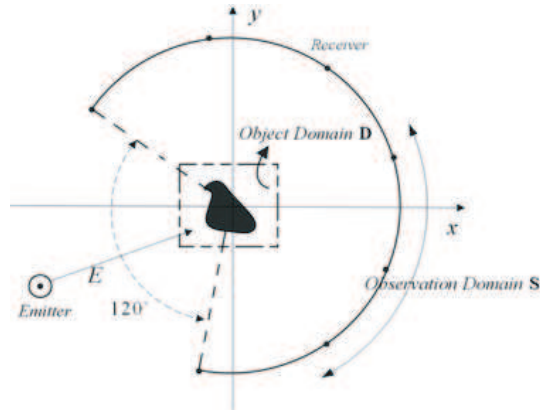
Figure 1. Geometrical model of the problem.

where $f_k(r)$ and $u_k(r)$ denote the total electric field in observation domain and investigation domain, respectively. k_b denotes the wavenumber of the homogeneous embedding and $u_k^{inc}(r)$ denotes the incident field in observation domain or object domain. $G(r, r')$ is the two-dimensional Green function of the background medium where r and r' are the position vectors. Here ω_k are the so-called contrast sources, defined as

$$\omega_k(r') = \chi(r') u_k(r') \tag{3}$$

where the contrast of the objects $\chi(r')$ is defined as $\chi(r') = k^2(r')/k_b^2 - 1$.

For simplicity, Equation (1) is rewritten in more condensed form using symbolic operator notation

$$f_k = u_k^{inc} + G_S \omega_k, \quad r \in S \tag{4}$$

where the operator is defined as

$$G_S \omega_k = k_b^2 \int_S G(r, r') \omega_k(r') \, dr' \quad r \in S \tag{5}$$

The state Equation (2), multiplying both sides of it with χ, can be expressed in symbolic form as

$$\omega_k = \chi u_k^{inc}, \quad r \in D \tag{6}$$

Introducing the following notations

$$f_{k,R} = \text{Re}(f_k), \quad f_{k,I} = \text{Im}(f_k), \quad u_{k,R}^{inc} = \text{Re}(u_k^{inc}), \quad u_{k,I}^{inc} = \text{Im}(u_k^{inc})$$
$$G_{S,R} = \text{Re}(G_S), \quad G_{S,I} = \text{Im}(G_S), \quad \omega_{k,R} = \text{Re}(\omega_k), \quad \omega_{k,I} = \text{Im}(\omega_k)$$

we can get the representation of (4) as

$$f_{k,R} = u_{k,R}^{inc} + G_{S,R}\omega_{k,R} - G_{S,I}\omega_{k,I} \text{ and } f_{k,I} = u_{k,I}^{inc} + G_{S,I}\omega_{k,R} + G_{S,R}\omega_{k,I}$$

As the PD-MRCSI method done, the PDB-MRCSI recasts the inversion problem as a minimization of a cost functional. Before introducing cost functional, we define $F(\omega_{k,n}, \chi_n)$ as a linear combination of the modified mismatch in data equation F_S and the mismatch in state equation F_D. Then the cost functional C can be expressed as

$$C(\omega_{k,n}, \chi_n) = F(\omega_{k,n}, \chi_n) F_{TV}(\chi_n) \qquad (7)$$

with

$$F(\omega_{k,n}, \chi_n) = F_S(\omega_{k,n}) + F_D(\omega_{k,n}, \chi_n)$$

$$F_S(\omega_{k,n}) = \eta_S \sum_k \left\| M_k^2 - f_{k,R}^2 - f_{k,I}^2 \right\|_S^2$$

$$F_D(\omega_{k,n}, \chi_n) = \eta_D \sum_k \left\| \chi u_k^{inc} - \omega_{k,n} \right\|_D^2$$

here M_k is the measured data, in particular, the amplitude of total wavefield distributed over the observed region; The subscript n denotes the index of iterative steps. The normalization factors are chosen as

$$\eta_S = \left(\sum_k \left\| |u_k^{inc}|^2 - M_k^2 \right\|_S^2 \right)^{-1} \text{ and } \eta_D = \left(\sum_k \left\| \chi_n u_k^{inc} \right\|_D^2 \right)^{-1}$$

where $\| \cdot \|_S^2$ and $\| \cdot \|_D^2$ denote the norm on $L^2(S)$ and $L^2(D)$, respectively.

In Equation (7), $F_{TV}(\chi_n)$ are the multiplicative regularized factor, i.e.,

$$F_{TV}(\chi_n) = \frac{1}{V} \int_D \frac{|\nabla \chi_n(r')|^2 + \delta_{n-1}^2}{|\nabla \chi_{n-1}(r')|^2 + \delta_{n-1}^2} dv(r') \qquad (8)$$

and $\delta_{n-1}^2 = F_{D,n-1}\tilde{\Delta}^2$, $\tilde{\Delta}$ denotes the reciprocal mesh size of the discretized domain D, V denotes the area of object domain D.

Then the inverse scattering problem can be solved by minimization the cost functional. The optimization procedure used in this paper is to update the two sequences (contrast sources and contrast) alternately using conjugate gradient method by minimizing the cost functional.

2.1. Updating the Contrast Sources

From Equation (8), we can see that the multiplicative regularized term $F_{TV}(\chi_{n-1})$ equals 1 at the beginning of each iteration; which means

we can only deal with the term F when updating the contrast sources $\omega_{k,n}$. Thereafter, the PDB-MRCSI starts with updating of the contrast sources ω_k in the following manner.

Define the modified data equation error and the state equation error to be

$$\rho_{k,n} = M_k^2 - f_{k,R,n}^2 - f_{k,I,n}^2 \text{ and } r_{k,n} = \chi_n u_{k,n}^{inc} - \omega_{k,n}$$

Supposing the contrast source and contrast in previous iteration, i.e., $\omega_{k,n-1}$ and χ_{n-1} are known, one can update ω_k by $\omega_{k,n} = \omega_{k,n-1} + \alpha_n^\omega v_{k,n}$, where α_n^ω is a real constant parameter to be determined by Equation (10). The update directions are chosen to be the Polak-Ribiere conjugate gradient directions

$$v_{k,n} = g_{k,n}^\omega + \frac{\text{Re} \sum_k \left\langle g_{k,n}^\omega, g_{k,n}^\omega - g_{k,n-1}^\omega \right\rangle_D}{\sum_k \left\langle g_{k,n-1}^\omega, g_{k,n-1}^\omega \right\rangle_D} v_{k,n-1}, \ n \geq 1 \text{ and } v_{k,n} = 0, \ n = 0$$

where $g_{k,n}^\omega$ is the gradient of the cost functional with respect to $\omega_{k,n}$ evaluated at $\omega_{k,n-1}$ and χ_{n-1}. Explicitly, the gradient for the updating of the contrast source is found to be

$$g_{k,n}^\omega = -2\eta_S \left[f_{k,n-1} G_S^* \right]^T \rho_{k,n-1} - \eta_{D,n} r_{k,n-1} \tag{9}$$

here G_S^* and χ_{n-1}^* are the complex conjugate of G_S and χ_{n-1}, respectively, and $[x]^T$ denotes transpose of $[x]$.

When the update directions are completely specified, the real parameter α_n^ω can be determined by

$$\alpha_n^\omega = \arg \min_{real \ \alpha} \left[F \left(\omega_{k,n-1} + \alpha v_{k,n}, \chi_{n-1} \right) \right] \tag{10}$$

where

$$
\begin{aligned}
& F \left(\omega_{k,n-1} + \alpha v_{k,n}, \chi_{n-1} \right) \\
&= F_S \left(\omega_{k,n-1} + \alpha v_{k,n-1} \right) + F_D \left(\omega_{k,n-1} + \alpha v_{k,n}, \chi_{n-1} \right) \\
&= \eta_S \sum_{i=0}^{4} A_i \alpha^i + \eta_D \sum_{i=0}^{2} B_i \alpha^i
\end{aligned}
$$

and the involved parameters are

$$
\begin{aligned}
A_0 &= \sum_k a_{0,k}^T a_{0,k}, & A_1 &= 2 \sum_k a_{0,k}^T a_{1,k}, \\
A_2 &= \sum_k \left(2 a_{0,k}^T a_{2,k} + a_{1,k}^T a_{1,k} \right), & A_3 &= 2 \sum_k a_{1,k}^T a_{2,k}, \\
A_4 &= \sum_k a_{2,k}^T a_{2,k}, & B_0 &= \sum_k \| p_{1,k} \|^2,
\end{aligned}
$$

$$B_1 = 2\sum_k Re\left(p_{1,k}^H p_{2,k}\right), \qquad B_2 = \sum_k \|p_{2,k}\|^2,$$

$$a_{0,k} = (f_{k,n-1,R})^2 + (f_{k,n-1,I})^2 - M_k^2,$$
$$a_{1,k} = 2\left[f_{k,n-1,R}\left(G_{S,R}v_{k,R,n} - G_{S,I}v_{k,I,n}\right)\right.$$
$$\left. + f_{k,n-1,I}\left(G_{S,R}v_{k,I,n} + G_{S,I}v_{k,R,n}\right)\right],$$
$$a_{2,k} = (G_{S,R}v_{k,R,n} - G_{S,I}v_{k,I,n})^2 + (G_{S,R}v_{k,I,n} + G_{S,I}v_{k,R,n})^2,$$
$$p_{1,k} = \chi_n u_k^{inc} - \omega_{k,n-1}, \qquad p_{2,k} = -v_{k,n}$$

Differentiation $F\left(\omega_{k,n-1} + \alpha v_{k,n}, \chi_{n-1}\right)$ with respect to α yields a cubic equation, explicitly,

$$\eta_S\left(4A_4\alpha^3 + 3A_3\alpha^2 + 2A_2\alpha + A_1\right) + \eta_D\left(2B_2\alpha + B_1\right) = 0 \qquad (11)$$

The real root is the desired minimizer α_n^ω.

2.2. Updating the Contrast

Using the same method, the contrast χ_n should be updated as

$$\chi_n = \chi_{n-1} + \beta_n^\chi d_n,$$

where d_n is the conjugate gradient direction and can be updated as

$$d_n = g_n^\chi + \gamma_n^\chi d_{n-1}$$

here γ_n^χ is the step length as

$$\gamma_n^\chi = \frac{Re\left\langle g_n^\chi, g_n^\chi - g_{n-1}^\chi\right\rangle_D}{\left\|g_{n-1}^\chi\right\|_D^2}$$

g_n^χ is the preconditioned gradient of the cost functional C with respect to χ_n evaluated at $\omega_{k,n}$ and χ_{n-1}, and is given by

$$g_n^\chi = \frac{g_n^D + g_n^{TV}F_{n-1}}{\sum_k |u_{k,n}|^2}$$

where g_n^D is the gradient of F_D with respect to χ_n, explicitly,

$$g_n^D = -n_{D,n-1}\sum_k\left(r_{k,n}u_{k,n}^*\right)$$

g_n^{TV} is the gradient of F_{TV} with respect to χ_n, explicitly,

$$g_n^{TV} = \frac{1}{2}\nabla \cdot \left[\frac{\nabla\chi_{n-1}}{|\nabla\chi_{n-1}|^2 + \delta_n^2}\right],$$

$u_{k,n}^*$ are the complex conjugate of $u_{k,n}$. After the updating directions are completely specified, the real parameter β_n^χ can be determined by

$$\beta_n^\chi = \underset{real\ \alpha}{\arg\min} \left[F_n\left(\omega_{k,n-1}, \chi_{n-1} + \beta_n d_n\right)\ F_n^{TV}\left(\chi_{n-1} + \beta_n d_n\right) \right] \quad (12)$$

Differentiation the term inside the square bracket of Equation (12) with respect to β yields a cubic equation and the real one is the desired minimizer β_n^χ.

3. NUMERICAL EXAMPLES

Three examples are given to validate the proposed algorithm in the present section. The geometrical model of the three examples is shown in Fig. 1, where an object domain D with size 17 cm by 17 cm is assumed.

The first case we consider is that of a single dielectric cylinder with radius 15 mm using the 2 GHz experimental data (filename: dielTM_dec8f.exp) provided by the Institut Fresnel, Marseille, France [21]. The parameters of the experimental setup needed for inversion as well as the database are described in the reference [21]. To sum it up briefly, the data correspond to $K = 36$ different source positions evenly distributed along a circle with radius 72 cm around the object domain, while $M = 36$ receivers are also evenly distributed along an observation domain with radius 76 cm which exits a blind zone of 120° angular section. The object domain D is discretized into 42×42 rectangular subdomains. The relative permittivity of this target is estimated to $\varepsilon_r = 3 \pm 0.3$ by an experimental method.
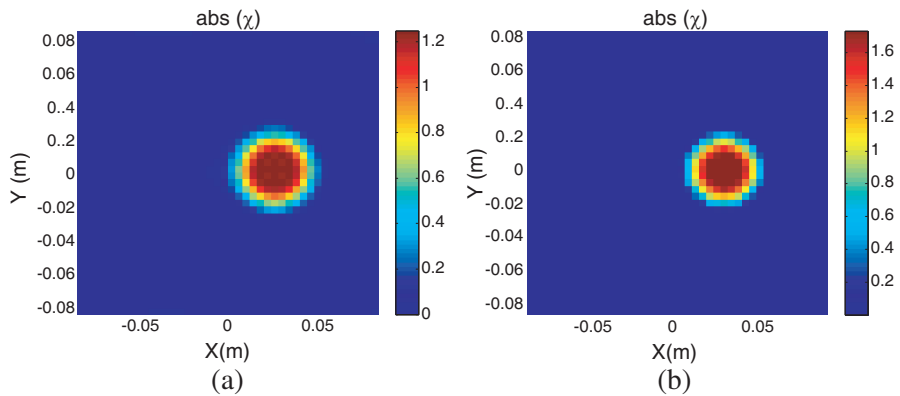
Figure 2. The reconstruction results of (a) PDB-MRCSI method, (b) PD-MRCSI method.
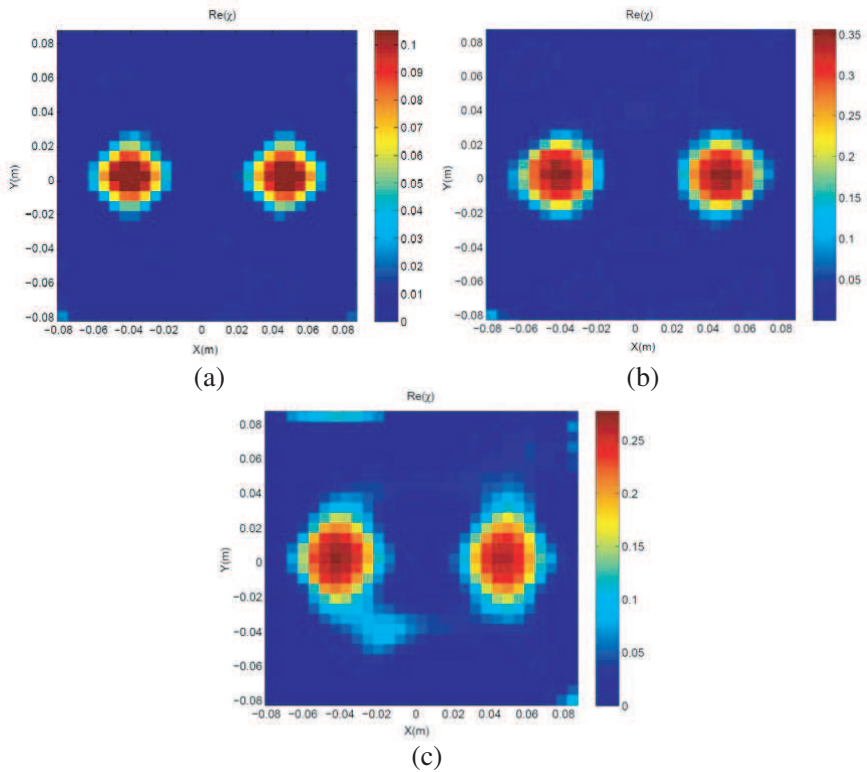
Figures 2(a) and 2(b) are the reconstruction results of PDB-MRCSI method and PD-MRCSI method, respectively. Both reconstructions are shown with 256 iterations since there is no obvious improvement observed on further iterations. From Fig. 2(a), we find that PDB-MRCSI method arrive at a fairly good reconstruction of location and shape of the object, while the achieved value of the contrast ($\chi = 1.22$) are slightly underestimated with respect to the expected value ($\chi = 2$). The outline of the reconstruction of PDB-MRCSI (radius equals 22 mm) is a little bigger than that of PD-MRCSI (radius equals 18 mm) shown in Fig. 2(b). With regard to the reconstruction time, the PD-MRCSI took 600.675 seconds for 256 iterations to get the satisfied results on a notepad computer with a Core2 T8100 2.1 GHz processor, while PDB-MRCSI only took 100.433 seconds. We can see that the time that PDB-MRCSI takes is almost one sixth of PD-MRCSI method. It is obviously that the algorithm we proposed reduces the computation time drastically. Although the reconstruction value of the proposed method is slightly underestimated with respect of PD-MRCSI, considering its good locating and shaping the objects, and low time cost, the PDB-MRCSI is a good inversion algorithm with phaseless data.

Although the Born approximation is incorporated in the proposed method, the PDB-MRCSI method is not limited to the case of weak scattering. Actually, the example above which $kd\chi \approx 2.51$ is not a case of weak scattering that should satisfied the $kd\chi \ll 1$, where d is the size of scattering object. The reconstruction results will be better for the weak scattering situations. The following example is presented to show empirically the largest $kd\chi$ that the method can still work for considered configuration.
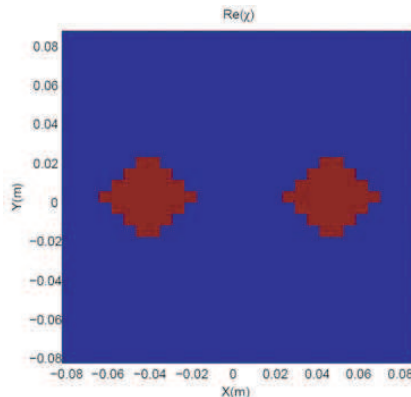
Figure 3. Original profile.

To conveniently adjust the contrasts χ, the synthetic data is used in this example. The geometrical model and parameters are not changed in this example, except that we use 25 emitters and 36 receivers in the new example. Two distinct square homogeneous cylinders of diameter 0.041 m separated from also 0.041 m are located in the object domain D which is discretized into 29×29 rectangular subdomains, see Fig. 3. The contrasts χ of the scattering objects are set to 0.1, 0.5 and 1.0 (i.e., $kd\chi = 0.4294,\ 2.1468,\ 4.2935$) to compare their reconstruction results. The reconstruction results are based on the synthetic data generated by solving the direct scattering problem with the help of CG-FFT approach. In order to satisfy the practical situation, we add 30% random white noise to the real and imaginary parts of the total field, respectively. Subsequently, the amplitudes of the total field are computed using the distorted data. The incident fields are chosen to be excited by line sources parallel to the axis of the scatterers and the frequency is 5 GHz.

Figure 4. The PDB-MRCSI reconstruction results with (a) $\chi = 0.1$, (b) $\chi = 0.5$ and (c) $\chi = 1.0$.

Figures 4(a)–(c) are the reconstruction results of PDB-MRCSI method with contrasts $\chi = 0.1, 0.5, 1.0$ ($kd\chi = 0.4294, 2.1468, 4.2935$), respectively. All the reconstructions are shown with 256 iterations since there is no obvious improvement observed on further iterations. From Fig. 4(a), ($kd\chi = 0.4294$), we find PDB-MRCSI method arrive at a fairly good reconstruction of location and shape and value of the object. In Fig. 4(b), ($kd\chi = 2.1468$), the location and shape of the objects are successfully reconstructed. However, the contrast of the object ($\chi = 0.35$) has been underestimated with respect to the actual value ($\chi = 0.5$). Additionally, there are some slight smears on the background. From Fig. 4(c), ($kd\chi = 4.2935$), we can see that the location and shape of the objects are well determined, while the outline are bigger than the actual target with long trail. As the contrast, the reconstructed value ($\chi = 0.27$) is almost one fourth of the actual value ($\chi = 1$). It is clear that as $kd\chi$ increases, the reconstruction results of PDB-MRCSI method become worse. It can be explained that although the PDB-MRCSI method is a good reconstruction algorithm, after all, it is a linear reconstruction method which can not solve the case far more than weak scattering ($kd\chi > 4.3$).

Since the PDB-MRCSI achieves a relatively good inversion results with low time cost, we take it as the initial estimate of PD-MRCSI method instead of back propagation method. It is called the combined method for convenience, and the two methods in the combined method are called PDB-part and PD-part.

The third example is presented to validate that using the combined method can dramatically reduce the computation time comparing to the PD-MRCSI method. To better describe the convergence of the problem, the synthetic data is also used in this example. The geometrical model and parameters are as same as the second example with $\chi = 0.5$. In this example, we also use the same method of the second example to add 30% random white noise to the amplitudes of total field.

The PDB-part optimization process in combined method will be terminated if one of the following stopping conditions is satisfied:

(1) The difference between the cost functional C at two successive iterates, n-th and $(n-1)$-th, is within a prescribed error quantity (it set to be 10^{-4})

(2) The total number of iterations exceeds a prescribed maximum $N_{\max} = 128$.

We also use ceasing criterion described above as the criterion of PD-part in combined method but changing the prescribed error quantity to 10^{-6} and changing the prescribed maximum to 256. The PD-MRCSI method which use back propagation method as its initial

estimate is also presented to compare with the combined method under the same ceasing criterion of PD-part.

In order to compare convergence effect of the methods proposed in this paper, we define the so-called "error in contrast" at iteration n as

$$ERR_{\chi_n} = \frac{\|\chi_n - \chi_{exact}\|_D}{\|\chi_{exact}\|_D}$$

where χ_n is the contrast distribution of the reconstructed profile at iteration n, and χ_{exact} is the exact one.

Figure 5 gives the reconstruction results of the combined method and PD-MRCSI method, respectively. From the figure, we can see that the reconstructed results of the combined method are almost as same as the PD-MRCSI method. It is easy to understand the phenomenon because the two methods have the same ceasing criterion. Fig. 6 shows the error contrast as function of the number of iterations using two methods, respectively. From Fig. 6, we can see there is an obvious break around 70 steps on the convergence line of combined method. Before the break, the PDB-part works; after that, the PD-part works. And from the Fig. 6, we can get that the PDB-part of combined method almost has the same convergence gradient with the PD-MRCSI method and the PD-part has a stable convergence gradient. What we focus about the combined method is the computation time. The combined method takes 74.90 s (163 steps) and the PD-MRCSI method takes 128.98 s (181 steps) on a notepad computer with a Core2 T8100 2.1 GHz processor, respectively. We can get that the combined method almost save half computation time of PD-MRCSI method. It can be concluded that when PDB-MRCSI serves as initial estimate, its fast convergence makes the combined method more effective.
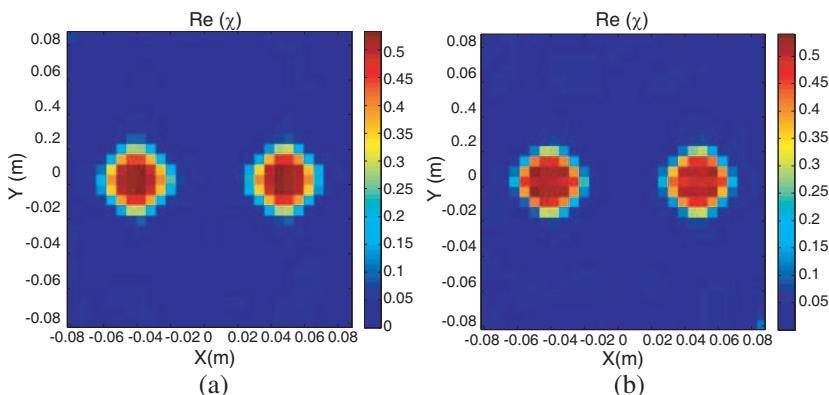
Figure 5. The reconstruction results of (a) the combined method, (b) PD-MRCSI method.
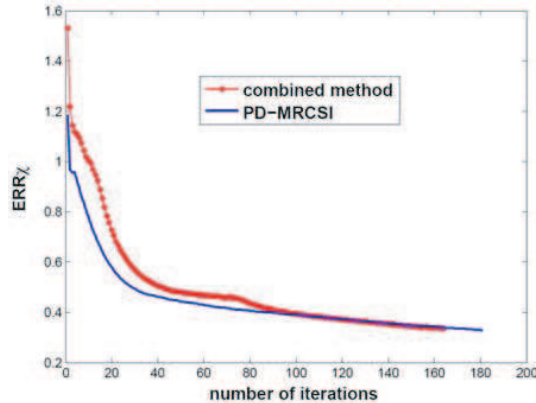
Figure 6. Error in contrast as function of the number of iterations using two methods.

4. CONCLUSION

In this paper, a novel electromagnetic inverse scattering algorithm has been proposed to solve the weak scattering problem with phaseless data. The algorithm has been proved to be a fast convergent and effective inversion algorithm for the weak scattering problem. Additionally, taking advantage of the properties of fast convergence of this method and stable convergence of PD-MRCSI method, the combined technique makes image reconstructions more fast and effective.

REFERENCES

1. Chew, W. C. and Y. M. Wang, "Reconstruction of two-dimensional permittivity distribution using the distorted Born iterative method," *IEEE Trans. Med. Imaging.,* Vol. 9, 218–225, 1990.

2. Zhang, Z. Q. and Q. H. Liu, "Two nonlinear inverse methods for electromagnetic induction measurements," *IEEE Trans. Geosci. Remote Sens.,* Vol. 39, 1331–1339, 2001.

3. Van den Berg, P. M. and R. E. Kleinman, "A contrast source inversion method," *Inverse Problems*, Vol. 13, 1607–1620, 1997.

4. Abubakar, A., T. M. Habashy, and P. M. van den Berg, "Nonlinear inversion of multi-frequency microwave Fresnel data using the

multiplicative regularized contrast source inversion," *Progress In Electromagnetics Research*, PIER 62, 193–201, 2006.

5. Abubakar, A., P. M. van den Berg, and S. Y. Semenov, "A robust iterative method for born inversion," *IEEE Trans. Geosci. Remote Sens.,* Vol. 42, 342–354, 2004.

6. Abubakar, A., P. M. van den Berg, and S. Y. Semenov, "Two- and three-dimensional algorithms for microwave imaging and inverse scattering," *Journal of Electromagnetic Waves and Applications*, Vol. 17, No. 2, 209–231, 2003.

7. Crocco, L. and T. Isernia, "Inverse scattering with real data: Detecting and imaging homogeneous dielectric objects," *Inverse Problems*, Vol. 17, 1573–1583, 2001.

8. Torresverdin, C. and T. M. Habashy, "Rapid 2.5-dimensional forward modeling and inversion via a new nonlinear scattering approximation," *Radio Sci.*, Vol. 29, 1051–1079, 1994.

9. Zhdanov, M. and G. Hursan, "3D electromagnetic inversion based on quasi-analytical approximation," *Inverse Problems*, Vol. 16, 1297–1322, 2000.

10. Guo, B., Y. Wang, J. Li, P. Stoica, and R. Wu, "Microwave imaging via adaptive beamforming methods for breast cancer detection," *Journal of Electromagnetic Waves and Applications,* Vol. 20, No. 1, 53–63, 2006.

11. Karanasiou, I. S., N. K. Uzunoglu, and A. Garetsos, "Electromagnetic analysis of a non-invasive 3D passive microwave imaging system," *Journal of Electromagnetic Waves and Applications,* Vol. 18, No. 3, 379–380, 2004.

12. Franceschini, G., M. Donelli, D. Franceschini, M. Benedetti, P. Rocca, and A. Massa, "Microwave imaging from amplitude-only data-advantages and open problems of a two-step multi-resolution strategy," *Progress In Electromagnetics Research*, PIER 83, 397–412, 2008.

13. Zhou, H., T. Takenaka, J. Johnson, and T. Tanaka, "A breast imaging model using microwaves and a time domain three dimensional reconstruction method," *Progress In Electromagnetics Research*, PIER 93, 57–70, 2009.

14. Dai, S. Y., C. Zhang, and Z.-S. Wu, "Electromagnetic scattering of objects above ground using MRTD/FDTD hybrid method," *Journal of Electromagnetic Waves and Applications*, Vol. 23, No. 16, 2187–2196, 2009.

15. Caorsi, S., A. Massa, M. Pastorino, and A. Randazzo, "Electromagnetic detection of dielectric scatterers using phaseless

synthetic and real data and the memetic algorithm," *IEEE Trans. Geosci. Remote Sens.*, Vol. 41, 2745–2753, 2003.

16. Litman, A. and K. Belkebir, "Two-dimensional inverse profiling problem using phaseless data," *J. Opt. Soc. Am. A*, Vol. 23, 2737–2746, 2006.

17. Crocco, L., M. D'Urso, and T. Isernia, "Faithful non-linear imaging from only-amplitude measurements of incident and total fields," *Optics Express*, Vol. 15, 3804–3815, 2007.

18. D'Urso, M., K. Belkebir, L. Crocco, T. Isernia, and A. Litman, "Phaseless imaging with experimental data: Facts and challenges," *J. Opt. Soc. Am. A*, Vol. 25, 271–281, 2008.

19. Zheng, H., L. Li, and F. Li, "A multi-frequency MRCSI algorithm with phaseless data," *Inverse Problems*, Vol. 25, 1–13, 2009.

20. Li, L. L., H. Zheng, and F. Li, "Two-dimensional contrast source inversion method with phaseless data: TM case," *IEEE Trans. Geosci. Remote Sens.*, Vol. 47, 1719–1736, 2009.

21. Belkebir, K. and M. Saillard, "Special section: Test inversion algorithms against experimental data," *Inverse Problems*, Vol. 17, 1565–1571, 2001.